Charge and Substituent Effects on Affinity and Metabolism of Benzbromarone-Based CYP2C19 Inhibitors

Charles W. Locuson, II,[†] Hisashi Suzuki,[‡] Allan E. Rettie,[§] and Jeffrey P. Jones[⊥,*]

School of Molecular Biosciences, Washington State University, Pullman, Washington, 99164, Meiji Seika Kaisha, Ltd., Pharmaceutical Research Center, Pharmacokin, 760 Morooka-cho, Kohoku-ku, Yokohama, Japan 222-8567, Department of Medicinal Chemistry, University of Washington, Box 357610, Seattle, Washington 98195-7610, and Department of Chemistry, Washington State University, P.O. Box 644630, Pullman, Washington 99164-4630

Received May 27, 2004

Human cytochrome P450 (CYP) 2C19 is one of the most important CYP2C family members responsible for metabolizing commonly prescribed drugs. This research describes synthetic modifications to benzbromarone (Bzbr) to create the most potent CYP2C19 inhibitor ever reported. The most important features enabling analogues of Bzbr to bind to CYP2C19 with high affinity are low acidity (high pK_a or nonionizability) and hydrophobic substituents adjacent to the phenol moiety. Though CYP2C19 was known to prefer neutral substrates, the extent was perhaps not realized until the anionic, parent compound Bzbr ($K_i = 3.7\ \mu$M) was compared to a less acidic dimethyl analogue ($K_i = 0.033\ \mu$M). However, differences in affinity for anionic and neutral Bzbr analogues did not appear to affect the regiospecificity of their metabolism by CYP's 2C19 and 2C9. In addition, some Bzbr analogues were metabolized both on the phenol and benzofuran rings. By using a substrate with a methyl ether in place of the Bzbr phenol, it was shown that some Bzbr analogues must be able to freely reposition after binding and oxidize the more energetically favorable position. Normally, *O*-demethylation of this methyl ether is favored over benzofuran hydroxylation based on ion current from LC/MS. Deuterium substitution of the methyl ether results in an inverse isotope effect on benzofuran hydroxylation (i.e. increased oxidation of this less favorable site). Likewise, Bzbr-based CoMFA models of CYP2C19 demonstrated no clear preference for any one ligand alignment. This suggests results from this modeling method must be interpreted carefully for each CYP isoform. In summary, Bzbr analogues have demonstrated they can be adapted to other CYP2C enzymes in order to probe isoform-specific properties.

Introduction

A superfamily of oxidative enzymes known as the cytochromes P450 are expressed in several tissues where they are utilized in both the biosynthesis of physiologically important metabolites and the biotransformation of foreign molecules, including drugs. Many of the drug metabolism reactions are catalyzed by P450s in the liver. By studying the specificity of these primarily hepatic isoforms, the ability to characterize the types of drug templates that possess high affinity for each P450 should improve. It is these compounds that could potentially interfere with the expected in vivo clearance of a second drug metabolized by the same isoform, thus leading to a drug interaction. Therefore, with some knowledge of a P450's pharmacophore, high-affinity P450 inhibitors can be identified and eliminated earlier in the drug design process to improve safety and lower the cost of development.

The CYP2C subfamily of P450s is particularly important in the metabolism of widely used drugs. For instance, 2C9 is known to metabolize acidic substrates such as the nonsteroidal antiinflammatory drugs (NSAIDs) and hypoglycemics (first and second generation sulfonylureas)[1] and is greatly inhibited by acidic compounds such as sulfaphenazole (SPA)[2,3] and benzbromarone (Bzbr).[4,5] CYP2C19, on the other hand, is a major oxidizer of omeprazole and (*S*)-mephenytoin[6] and is subject to inhibition by potent *N*-3-benzyl derivatives of nirvanol and phenobarbital,[7] all of which are primarily neutral at physiological pH. Thus, it appears 2C19 lacks the strong preference for anions. The fact that these two enzymes are 91% identical at the protein level raises an interesting question regarding specificity. How do the 43 differing amino acid residues between the two enzymes work in concert to confer preference for some substrates over others? This is a biochemical question that has clinical implications. These enzymes' variant alleles lead to altered pharmacokinetics for proton pump inhibitors (PPIs), mephenytoin, phenytoin, and tricyclic antidepressants and therefore, at some dosage levels, efficacy and safety (reviewed in Desta et al.[8]).

Recently, we have demonstrated that the potent 2C9 Bzbr inhibitors derive part of their affinity from existing in their anionic phenolate form at physiological pH. Remarkably, 2C19 appears to lack such a preference even though many of the active site residues are conserved between 2C19 and 2C9 as predicted by Gotoh's sequence alignments.[9] Mutation of a few 2C9 residues and construction of 2C9 chimeras with larger

* To whom correspondence should be addressed. Tel: (509)-335−5983. Fax: (509)-335-8867. E-mail: joswigjones@earthlink.net.
† School of Molecular Biosciences, Washington State University.
‡ Meiji Seika Kaisha, Ltd.
§ University of Washington.
⊥ Department of Chemistry, Washington State University.

10.1021/jm049605m CCC: $27.50
Published on Web 11/26/2004

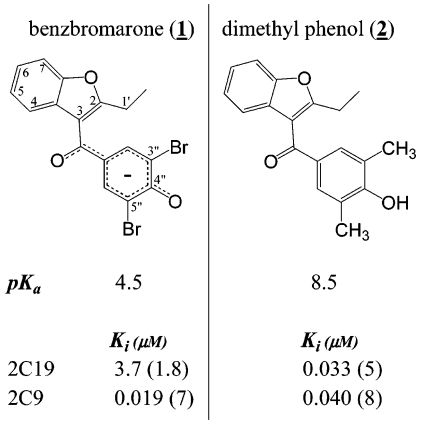

Figure 1. Effect of pK_a on 2C19 inhibition by parent compound benzbromarone and a less acidic analogue. The numbering scheme of Bzbr follows De Vries et al..[24] The number in parentheses after the K_i value represents the error associated with the last significant figure.

2C19 substitutions begins to confer similar, but not identical activity, to that of 2C19.[10,11] To test the role of substrate charge for 2C19, both neutral and acidic analogues of the potent 2C9 inhibitor Bzbr were screened for their relative affinity. As with 2C9, the Bzbr analogues with two hydrophobic groups on the benzoyl ring were greatly preferred by 2C19; however, in contrast to Bzbr's affinity for 2C9, the compounds with these hydrophobic groups were better 2C19 inhibitors when they were neutral or contained less acidic phenols than Bzbr. This is surprising since a key Arg residue (R108) in 2C9 implicated in binding anionic substrates is also present in 2C19.[12] The best 2C19 inhibitor identified here most closely resembled Bzbr, but had a much less acidic phenol (pK_a of 8.5 versus 4.5). This dimethylphenol analogue ((2-ethylbenzofuran-3-yl)−(4-hydroxy-3,5-dimethylphenyl)methanone) is the most potent 2C19 inhibitor thus far described ($K_i = 0.033\ \mu$M) and demonstrates the importance of this class of compounds in exploring the subtle structural differences between 2C19 and 2C9.

Results

Inhibition of 3-*O*-Methylfluorescein Demethylation by 2C19. All Bzbr analogue inhibitors (Figure 1 and Table 1) were found to be competitive inhibitors of methylfluorescein turnover by recombinant, reconstituted 2C19 according to nonlinear least-squares fitting results from EnzFitter 2.0 shown in Figure 2 (BIOSOFT, Ferguson, MO). 2C19's V_m and K_m for methylfluorescein demethylation was 1.5 nmol/min/nmol and 5.9 μM, respectively.

Comparison of Relative Affinities. The best inhibitors of 3-*O*-methylfluorescein turnover by 2C19 were, by far, those that retained the closest structural similarity to the parent compound Bzbr, but were less acidic than Bzbr (Table 1). All five of these compounds had K_i values in the nanomolar range. This includes the dimethylphenol analogue **2** where the only difference from Bzbr is the substitution of methyl groups for two bromine atoms (Figure 1). By substituting the electron-withdrawing bromines with methyl groups of nearly the same van der Waals radii, the pK_a of the phenol group increases nearly 4 log units to 8.6. This ensures the protonated form of this compound dominates under the in vitro incubation conditions used (pH = 7.4). This dimethylphenol is the most potent 2C19 inhibitor described to date. Likewise, the next four most effective 2C19 inhibitors either had higher phenol pK_as relative to Bzbr, or methylated phenols. When the Bzbr ketone is reduced to the racemic alcohol **4** or the phenol ring is isolated from the ketone with a methylene group (**6**),

Table 1. Benzbromarone Analogs Screened for Inhibitory Potency against 2C19, or Used as Substrates or Metabolite Standards

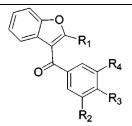

comp	K_i (μM)[a]	pK_a	R_1	R_2	R_3	R_4
3	0.25 (5)	NA	-CH_2-CH_3	-CH_3	-O-CH_3	-CH_3
4	0.30 (8)	8.8	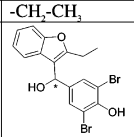			
5	0.37 (9)	NA	-CH_2-CH_3	-Br	-O-CH_3	-Br
6	1.6 (4)	8.6	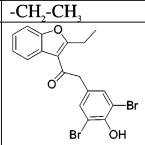			
7	1.6 (4)	5.2	-CH_2-CH_2-CH_2-	-Br	-OH	-Br
8	2.4 (7)	ND	-CH_3	-Br	-OH	-Br
9	2.5 (6)	8.4	-CH_3	-H	-OH	-H
10	3.7 (7)	NA	-CH_2-CH_3	-H	-N-$(CH_3)_2$	-H
11	4.5 (8)	8.4	-CH_3	-OH	-H	-H
12	4.5 (1.2)	NA	-CH_3	-H	-O-CH_3	-H
13	7.2 (1.8)	5.2	-CH_3	-I	-OH	-I
14	13 (2)	NA	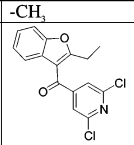			
15	13 (5)	NA	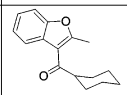			
16	substrate		-CH_3	-O-CH_3	-H	-H
17	substrate		-CH_3	-OC^2H_3	-H	-H
18	metabolite standard, not detected			-Br	-OH	-Br

[a] The number in parentheses after the K_i value represents the error associated with the last significant figure.

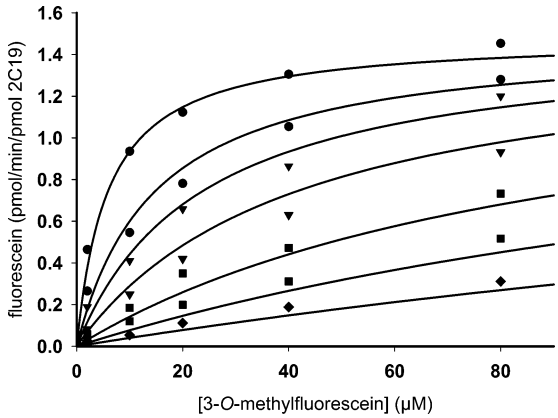

Figure 2. Dimethylphenol analogue **2** inhibition of 2C19-mediated 3-*O*-methylfluorescein turnover shown with the nonlinear fit to the competitive inhibition equation.

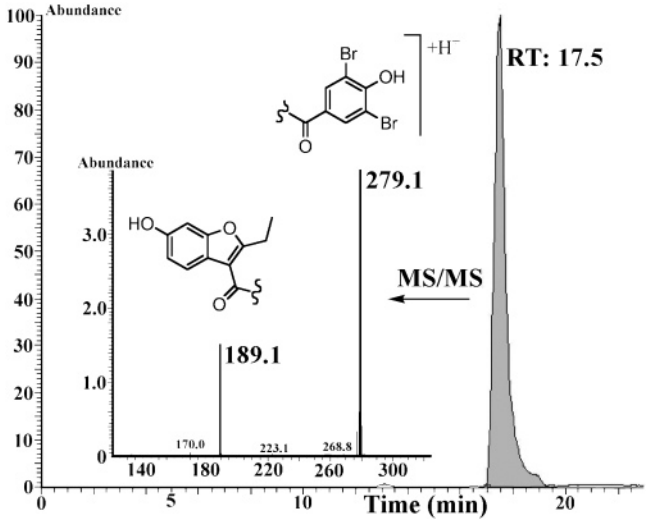

Figure 3. Selected ion mass chromatogram at *m/z* 441.2 (substrate + 16) and MS/MS data (inset) resulting from Bzbr metabolism by 2C19. An identical profile was observed for 2C9.

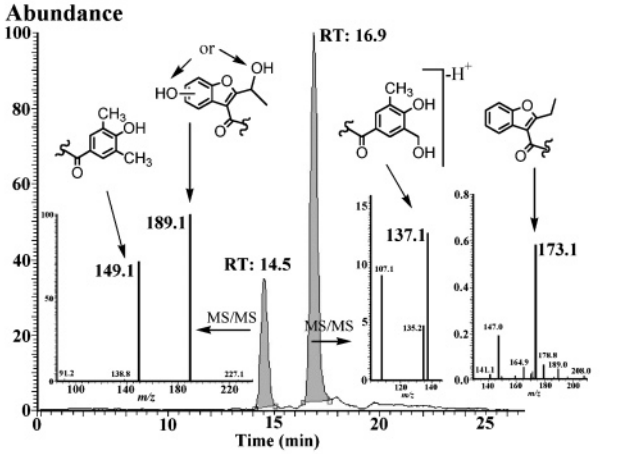

Figure 4. Selected ion mass chromatogram (substrate + 16) and MS/MS data (inset) resulting from metabolism of the dimethylphenol analogue **2** by 2C19. Two major hydroxylation products were observed, but they reside on different ends of the molecule.

the pK_a exceeds 8.5. Methylating compound **2** to obtain **3** and methylating Bzbr itself (**5**) also provides more potent 2C19 inhibitors than any of the anionic derivatives.

The trend for 2C19 in preferring neutral Bzbr analogues is opposite to the trend observed with the same compounds that were screened for inhibition toward 2C9[13] because in every case, the anionic Bzbr analogues have the highest affinity for 2C9 (e.g. **1**, **7**, **8**, **13**). Conversely, the less acidic compounds **2**−**6** are only slightly poorer inhibitors of 2C9 than the anionic derivatives; however, with 2C19, **2**−**6** give K_i values at least an order of magnitude lower than the anionic compounds **1**, **7**, **8**, **13** on average. In fact, the 100-fold difference in K_is between Bzbr (**1**) and the less acidic dimethylphenol **2** is one of the most striking effects of charge observed among 2C19 ligands (Figure 1). Despite this trend, all but two of the inhibitors (**2**, **3**) are more active toward inhibiting 2C9 relative to 2C19.

The remaining Bzbr analogues tested substituent effects and their locations on the benzoyl ring. Mirroring the 2C9 results, 2C19 preferred the phenol group at the C-4" position (para to the ketone; analogue **9**) over a methoxy group at the same position (**12**) or a phenol at the C-3" position (**11**). The poorest 2C9 inhibitor (**14**) was also one of the poorest 2C19 inhibitors. This substituted pyridine-containing structure contains two halogens in the same positions as Bzbr, but has a nitrogen in the ring where the Bzbr phenol is located. One of the biggest differences between 2C19 and 2C9 was also noted with the cyclohexane-containing analogue **15**. Compound **15** was an equally poor inhibitor of 2C19 as the pyridine derivative, whereas the same compound was better than seven other compounds screened against 2C9.

Metabolism of Bzbr (1) and Its Dimethyl (2) and 3″-Methoxy (16, 17) Analogues. Both Bzbr and its dimethyl analogue appear to be metabolized to the same products by 2C19 and 2C9 as judged by retention times and fragmentation patterns. Only one Bzbr metabolite was detected with both enzymes, and it had a retention time of 17.5 min (Figure 3). This metabolite is hydroxylated on the benzofuran as evidenced by the *m/z* of the two fragments. The fragment with an *m/z* of 279.1 represents the unmodified benzoyl phenol ring. It also clearly possesses the bromine isotope pattern when the parent ion *m/z* window is increased. The second most abundant fragment (*m/z* = 189.1) represents 2-ethylbenzofuran plus 16 mass units, or a hydroxylated benzofuran. Hydroxylation could occur at one of four aromatic positions or the C-2 ethyl group. On the basis of differences in chromatographic retention times and fragmentation patterns of our synthesized standard 1′-OH Bzbr, hydroxylation does not appear to occur on the C-2 ethyl group. The 1′-OH metabolite standard eluted 0.8 min earlier under the chromatography method. In positive mode, this standard also appeared to lose water at the allylic position (*m/z* = 422.9) and form an adduct (*m/z* = 454.5) where the product from enzyme incubations gave only the expected M + 1 ion (*m/z* = 441.2). Both the 1′-OH metabolite standard and the product from enzyme incubations gave the expected M − 1 ion in negative polarity mode, but MS/MS results showed major differences (data not shown). No evidence was seen for multiple hydroxylations of the substrate.

The dimethylphenol analogue **2** formed two hydroxylated metabolites (M + 16) of retention times 14.5 and 16.9 min with 2C19 and 2C9 (Figure 4). Analyte from the first peak to elute fragmented at the ketone to give the unmodified dimethylbenzoylphenol ring (*m/z* = 149.1) and a hydroxylated 2-ethyl benzofuran (*m/z* = 189.1) similar to the Bzbr results. The primary daughter ion of the second hydroxylation product to elute had an *m/z* corresponding to M − 18 suggesting water loss. At lower *m/z* values, fragments for an unmodified benzofuran ring (*m/z* = 173.1) and a hydroxylated dimethylphenol ring (*m/z* = 137.1) were found. Together, these results would place the site of hydroxylation at one of two benzylic positions on the phenol ring.

Two readily distinguishable metabolites of **16** were also observed in 2C19 and 2C9 incubations. At a RT of 17.6 min, MS/MS provided a fragment corresponding to a hydroxylated benzofuran (*m/z* = 175.1) and another for the 3″-methoxy ring (*m/z* = 135.0). The second product at 19.2 min was found to be an *O*-demethylation product that eluted with the same RT as compound **11**

and displayed the same fragmentation pattern. Its fragments matched the *m/z* values of an unmodified benzofuran (*m/z* = 159.1) and a benzoyl phenol ring (*m/z* = 121.0).

To probe the extent of substrate mobility after binding to 2C19, **11** was deuterated to make analogue **17**, which differs from **16** only at the isotope-labled 3″-methoxy group. Analogue **17** gave the same two products as **16** with the addition of 3 Da to the methoxy-d_3 ring. The ratio of the two products, however, differed significantly relative to the protio version (Table 1). A normal isotope effect where more *O*-demethylation occurs with the protio than the deutero analogue was observed for *O*-demethylation, and a corresponding inverse isotope effect was observed for benzofuran hydroxylation. The presence of an inverse isotope effect infers two possibilities. One is that the substrate retains high mobility after binding, assuming limited dissociation. Alternatively, the presence of another bound substrate may allow branching to this second molecule if it can approach the heme.[14] All product ratios remained constant after addition of the dimethylphenol **2** substrate to incubations containing the methoxy analogue, suggesting the isotope effects do not result from multiple substrate binding.

Comparative Molecular Field Analysis Modeling (CoMFA). No validated models could be generated using the 15 Bzbr analogues as evidenced by negative q^2 values. While this is a small data set, the same compounds produced models with error below 0.5 *ln* units using 2C9-derived K_i values.[13] Since charged analogues were among some of the poorest inhibitors of 2C19, the atomic partial charges of those with pK_as lower than 5.2 (**7**, **8**, **13**) were recalculated with a charge of −1 after the phenol proton was removed. The resulting models could not correlate ligand charges with their associated K_i values.

To increase the diversity of the data set, the Bzbr analogues were added to our recently described model of 24 phenobarbital, nirvanol, and phenytoin derivatives (in press).[15] After this merging, cross-validated models were readily generated, but were largely independent of how Bzbr was aligned (Figure 5). Model statistics remained mostly unchanged for all four alignments with cross-validated q^2 values and standard errors (*ln* units) averaging 0.64 and 0.89, respectively.

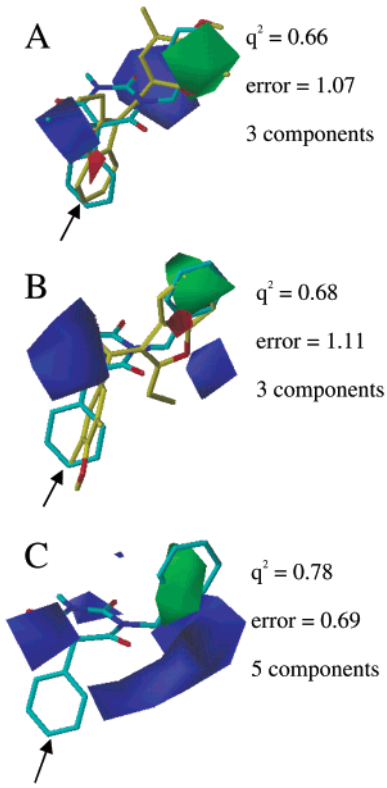

Figure 5. Bzbr CoMFA model contours for 2C19 were similar for multiple ligand alignments to phenobarbitals and not much different from the phenobarbital model lacking Bzbr. Arrow denotes site of metabolism of (−)-*N*-3-benzylphenobarbital and proposed sites of metabolism of **2**. (a) Alignment of the Bzbr benzofuran to the metabolized position of (−)-*N*-3-benzylphenobarbital. (b) Alignment of the dimethylphenol **2** metabolized benzylic position to the metabolized position of (−)-*N*-3-benzylphenobarbital. (c) Phenobarbital/nirvanol/phenytoin model without Bzbr analogues.

Discussion

Five of the Bzbr analogues described here exhibit extraordinary inhibitory potency for 2C19 with their submicromolar K_i values. Therefore, as arguably some of the most complementary ligands for the 2C19 active site, Bzbr analogues should answer many questions regarding 2C19 specificity. For example, this is the first report of a series of closely related compounds that demonstrate the charge state of a substrate could determine whether it is a micromolar or a low nanomolar inhibitor of 2C19 (Figure 1). Since Bzbr was initially found to be a 2C9 inhibitor, this work also shows the Bzbr-like compounds can be altered to exploit other 2C enzymes as was done with the dimethyl sulfaphenazole analogue DMZ.[16]

Features of the Best Bzbr 2C19 Inhibitors. Structures with the highest resemblance to the parent compound Bzbr (**2**−**6**), but with decreased acidity, possessed the best affinity for 2C19 as judged by K_i values (Figure 1 and Table 1). Acidity was adjusted in two ways. In some cases the ionizable phenol was simply blocked with a methyl group as in **3** and **5**. Alternatively, the benzoyl ring substituents were altered to diminish their electron-withdrawing capacity as in **2**, **4**, and **6**. More than one hydrophobic group on the phenol ring was just as essential for 2C19 affinity. Shuffling of single benzoyl ring substituents to different positions did not improve their inhibitory capability even though they had low acidity. Therefore, all three of Bzbr's benzoyl ring substituents at C-3″, -4″, and -5″ are required for optimal binding to 2C19 with a nonacidic phenol favored over methoxy at C-4″. At the benzofuran ring, substitutions were only made to the length of the C-2 alkyl chain. No correlation in K_i values was witnessed between chain lengths ranging from one to four carbons in compounds **1**, **7**, and **8**, suggesting the higher negative charge of these acidic derivatives makes them equally weaker binders.

These findings would appear to agree with 2C9's favorite benzoyl ring substituents, but contrast 2C9's ability to bind both anionic and neutral Bzbrs with nearly equal affinity. When the less acidic dimethylphenol **2** was screened for its ability to inhibit (*S*)-warfarin metabolism by 2C9, it was nearly as potent (K_i = 40 nM) as anionic Bzbr (K_i = 19 nM). This demonstrates

that given the same steric properties, requirements for charge state in 2C9 substrates are not very stringent. In fact, this turned out to be a general trend in most of the Bzbr analogues screened against 2C9. Hence, the same C-3″, -4″, and -5″ substituents probably make favorable interactions with both enzymes while 2C19 is much more intolerant of substrates with a formal negative charge under physiological pH.

Comparison of Bzbr with Other 2C19 Substrates. The higher-affinity 2C19 substrates that are larger than (*S*)-mephenytoin all share similar features. Bzbr, the *N*-benzylphenobarbitals, and sulfoxide-containing proton pump inhibitors (e.g. omeprazole) all have an aromatic or benzylic position that is metabolized, separated from a second aromatic/hydrophobic group by a polar, bridging group such as a ketone or sulfoxide (Figure 6). On the basis of these findings, 2C19 would appear to make an H-bond or electrostatic interaction with the polar, bridging group and a hydrophobic/aromatic interaction further beyond the heme. Proton pump inhibitors suggest a direct enzyme interaction with the polar bridging group. The regiospecific metabolism of omeprazole is primarily determined by its chiral sulfoxide in 2C19 [17] whereas lansoprazole displays a change in affinity for 2C19 dependent upon the chirality of its sulfoxide.[18] Unfortunately, specific residue(s), not including backbone interactions, cannot be easily singled out from the recent 2C9 structures [19] because the two most apparent choices based on their location in 2C9, R108 and H99, have outward facing side chains. However, recent evidence for the flexibility of the B′−C loop in 2C9 [12] could make these residues candidates for 2C19−substrate interactions either during substrate recruitment or during catalysis. H99 is intriguing because it is one of the closest residues to the heme that is different from 2C9. This histidine is already known to be a major source of 2C19's ability to metabolize omeprazole by presumably donating an H-bond to its sulfoxide.[10]

Previous 2C19 homology models [20−22] and chimera studies [11,22,23] have determined the general localities of residues further from the heme that make 2C19 unique based on mutagenesis. These residues presumably affect enzyme motion during substrate binding or protein−protein interactions. Further speculations regarding the roles of all 2C19 residues that differ from 2C9 can be found in the literature for the F−G loop and B′−C loop regions [10] and the I- and G-helix regions.[11,22,23]

CoMFA Models. Bzbr analogues were added to 24 phenobarbital analogues to carry out CoMFA because the Bzbr analogues were too limited to derive models. Unexpectedly, this combination of compounds generated CoMFA models with moderate to high q^2 values ($0.5 < q^2 < 0.7$) for all four ways in which Bzbr was aligned to the *N*-substituted phenobarbitals (Figure 5). The models, then, appear inconclusive because there is no way to determine which one is more correct. For instance, the two most logical alignments are the overlap of either the benzofuran C-6 metabolized position or phenol ring with that of the phenobarbital metabolized position (C-5 phenyl ring),[15] and alignment of the other two rings. Yet the q^2 values and standard errors are comparable and a similar set of three-dimensional electrostatic and steric interactions are found in the two contour plots

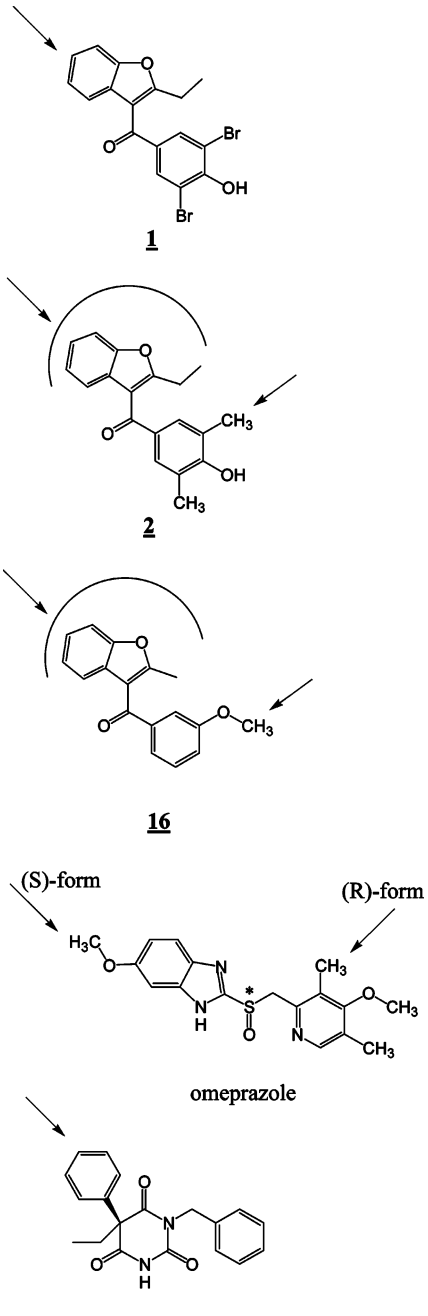

Figure 6. Sites of oxidation of Bzbr analogues by 2C19 compared to the substrates omeprazole [17] and (−)-*N*-3-benzylphenobarbital.[15]

(Figure 5). Therefore, all models are either correct to different extents, or provide almost no insight into potential enzyme-ligand interactions.

The lack of more concrete CoMFA results can be explained by two scenarios. Scenario number one is that the data set is too limited. After reviewing the compounds, it appears that the difficulty in modeling 2C19 using CoMFA could arise from the lack of sufficient chemical diversity in the Bzbr compounds. Bzbr analogues are clearly lacking in modifications to the benzofuran group. Plus, the contour plot features for the phenobarbital model do not change much after addition of the Bzbrs. Both models contain prominent, favorable electropositive (blue) and steric interaction (green) sites near C-5 and the *N*-benzyl group of the phenobarbital

barbiturate ring, respectively (Figure 5). C-5 lies above the aromatic rings that are metabolized in both classes of compounds, and the hydrophobic *N*-benzyl group aligns with whichever Bzbr ring is not positioned for metabolism.

The second scenario is that there is no single substrate conformation that is greatly favored over another for Bzbr analogues. A single P450 isoform is often capable of metabolizing multiple positions on a substrate, but orienting substrates toward their primary oxidation site in CoMFA modeling has proven viable in the past for 2C9. Obviously, alignments used to generate QSARs, even with the aid of active site docking, must be carefully tested before any conclusions are drawn based on statistically validated models.

Metabolism of Bzbr and Its Analogues. To test whether the CoMFA data set does not fully explore all enzyme−substrate interactions or if more than one favorable binding conformation is populated, metabolism studies were carried out on select Bzbr analogues. The metabolism of Bzbr by 2C19 and 2C9 was studied using LC/MS/MS. Previously, microsomal incubations and human subject samples have allowed the characterization of several Bzbr metabolites with the primary hydroxylated products being 6-OH and 1′-OH Bzbr in a ratio of 6:1, respectively.[24] It is reported here that 2C19 and 2C9 are involved in forming the 6-OH Bzbr metabolite.[24] Though NMR was not used to assign the 6-OH position as done previously by purifying it from human urine,[24] the product possessed a different retention time (17.5 versus 16.7 min) and fragmentation pattern than the synthesized 1′-OH metabolite, **18**. While these findings are largely qualitative, this is the first report demonstrating the hydroxylation of Bzbr in a nonmicrosomal, in vitro system.

The metabolism of Bzbr analogues **2** and **16** mirrors that of omeprazole where either hydrophobic end can approach the heme (Figure 6). Bzbr is metabolized at the aromatic C-6 of the benzofuran by both 2C19 and 2C9, but due to the presence of two bromines, the phenol ring is unavailable for oxidation. On the other hand, metabolism of the dimethylphenol **2** and **16** demonstrate their ability to bind in alternate conformations. In addition to an unidentified benzofuran metabolite, the dimethylphenol **2** is also converted to a benzyl alcohol metabolite whereas **16** is *O*-demethylated to give **11**. Therefore, both of these analogues show how Bzbr analogues can bind in more than one conformation where the sites of metabolism are at each end as in omeprazole.[17]

This challenges the hypothesis that the bromine and methyl group phenol ring substituents interact at a site somewhat removed from the heme. Due to the large effects bromination and methylation of the phenol ring have on 2C19 affinity, a complementary hydrophobic pocket in the active site seemed likely. Other evidence for this is that 2C9 appears to prefer these hydrophobic groups for interactions at specific enzyme sites and is not just a result of poorer water solubility.[13] Certain scenarios involving favorable hydrophobic pockets both near the heme and further from the heme near the nonmetabolized position can be envisioned; however, another consideration is that of energetics. In the cases of the dimethylphenol **2** and **16**, the phenol ring benzylic and methoxy metabolized positions are easier to oxidize than the aromatic position on the benzofuran.[25]

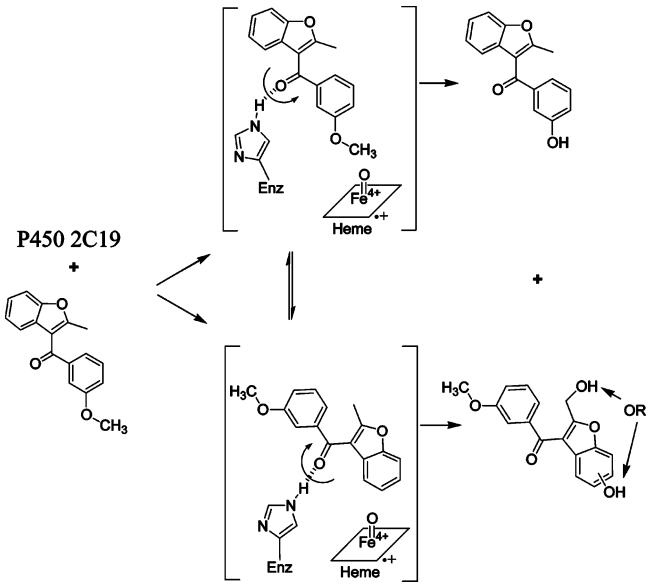

Figure 7. Isotope effects on metabolism of the 3″-methoxy analogue **16** suggest there is rapid switching of substrate conformations after binding to 2C19. Both ring systems are capable of colliding with the reactive oxygen species at the heme; therefore, it is possible the binding site for Bzbr analogues may have a hydrophobic or aromatic region that interacts equally well with the substrate rings, or a H-bond donor (e.g. H99) that allows it to pivot at the ketone.

Table 2. Kinetic Isotope Effects on Metabolism of Analogue **16** by 2C19

product[a]	$k_H/k_{D\ obsd}$[b]
O-demethylation	2.6 ± 0.3
benzofuran hydroxylation	0.34 ± 0.05

[a] Characterized by LC/MS/MS. [b] Selected ion current of protio and deutero analogue products corrected to internal standard and divided by each other. Enzyme incubations were performed in triplicate.

To test whether Bzbrs are able to switch conformations after binding, or if the way they enter the enzyme determines their metabolism, an isotope effect experiment was performed. Compound **11** was deuterated with iodomethane-$^2H_3$ to give **17**, incubated with 2C19, and the results compared with nonlabeled **16**. Though hydrogen atom abstraction during P450 catalysis is not rate limiting, isotope effects are observable when a substrate is able to switch conformations so that a different position on the substrate is metabolized.[25−27] A simplified scheme for this branching effect as proposed by Miwa et al.[28] is represented in Figure 7. *O*-Demethylation is made more difficult by substituting deuteriums, so an increase in the benzofuran metabolite would signify the equilibrium population of the enzyme−substrate complex that gives the benzofuran metabolite increases, and this is what was found. An observed kinetic isotope effect ($k_H/k_{D\ obs}$) of 2.6 for *O*-demethylation was noted (Table 2). Not only did *O*-demethylation decrease, but benzofuran hydroxylation increased to give an observed inverse isotope effect of 0.34. If only *O*-demethylation decreased relative to the internal standard, then this may indicate that the enzyme only branches to the nonproductive shunt pathways; however, the witnessed isotope effects suggest there are

Table 3. Product Ratios of Substrates **16** and **2** Observed with 2C19 Separately and with Each Other

substrate(s)	product ratio of **16**[a] *O*-demethylation to benzofuran hydroxylation	product ratio of **2** benzylic hydroxylation to benzofuran hydroxylation
16	2.8 ± 0.2	-
2	-	7.9 ± 0.5
16 + **2**	2.8 ± 0.2	7.5 ± 0.2

[a] Product ratios from enzyme incubations performed in triplicate based on selected ion current.

multiple enzyme−substrate intermediates that interchange more rapidly than bond scission occurs. The intrinsic isotope effect, which can be thought of as the maximal isotope effect, can be estimated assuming product branching [29] and irreversible substrate binding.[28] If the products' $k_H/k_{D\ obs}$ ratios are divided, a value of 7.6 is obtained as the intrinsic isotope effect estimate.[29] This value is near what would be observed for a substrate that has unhindered mobility within the enzyme.[30]

An alternative explanation is the simultaneous occupation of a P450 active site by multiple substrates where each molecule has the opportunity to collide with the heme oxidizing species. If one molecule binds with the methoxy group near the heme and a second molecule binds with the benzofuran near the heme, then deuterium labeling would still allow branching to the benzofuran metabolite. This was first observed by Rock et al. in fatty acid metabolism by P450 BM-3.[14] Therefore, the similar dimethylphenol substrate **2**, which is also metabolized at two positions, was added to 2C19 incubations with the methoxy analogue. Product ratios for both substrates did not change (Table 3) indicating, but not definitively ruling out, that one substrate binds per catalytic turnover.

In summary, metabolic studies of Bzbr analogues show for the first time that 2C19 regiospecificity is not necessarily dictated by the orientation in which substrate enters the enzyme. Figure 7 illustrates how enzyme−substrate complexes exist at equilibrium after binding to oxidize positions that are several angstroms removed. On the basis of these and other current findings, two kinds of enzyme−substrate interactions could be proposed. First is the stereochemically sensitive metabolism of proton pump inhibitors that is driven by sulfoxide chirality. Since the Bzbr analogues are also metabolized on multiple rings separated by a ketone, a polar group may act as a pivot point for substrate branching. The second observation is that *N*-benzyl substitution of phenobarbital increases its affinity into the low nanomolar K_i range. Therefore, hydrophobic or aromatic interactions with substrate could be made with either ring system so that one of the rings is always placed above the heme.

Conclusions

The findings presented here demonstrate the increased utility of benzbromarone analogues since they have now been adapted to make the best 2C19 inhibitor reported. Because P450s accommodate many substrates, having high-affinity ligands should prove useful in describing the most favorable enzyme−substrate interactions based on their complementary features. This is important for drug design from the standpoint of avoiding drug−drug interactions and understanding the molecular effects of point mutations resulting from variant P450 genes. For 2C19, ligands with two hydrophobic regions separated by a polar group are the most complementary according to this study with benzbromarone and previous works on phenobarbital analogues and proton pump inhibitors. Particularly intriguing is that high-affinity binding of benzbromarone ligands to 2C19 appears to be achieved without constraining substrate mobility within the enzyme. This mobility allows each hydrophobic end of the substrate to approach the heme for oxidation and is likely the reason QSAR modeling, although statistically successful, could not be evaluated objectively.

Materials and Methods

Chemicals. Fluorescein, 3-*O*-methylfluorescein, dichlorofluorescein, regenerating system components, and all biochemicals were obtained from Sigma-Aldrich (St. Louis, MO). Solvents were purchased from J. T. Baker (Phillipsburg, NJ). Fine chemicals were from Aldrich (Milwaukee, WI). Iodomethane was purchased from Cambridge Isotope Laboratories (Andover, MA). Warfarin and 4′OH-warfarin were gifts from Prof. W. F. Trager at the University of Washington (Department of Medicinal Chemistry).

Enzyme Sources. Purified, full-length human 2C19 was kindly provided by Prof. A. E. Rettie at the University of Washington (Department of Medicinal Chemistry). Details of cDNA subcloning, expression in *Trichoplusia ni* cells, and purification can be found in Suzuki et al.[7] Bacterial expression and purification of cytochrome P450 reductase and cytochrome b5 were carried out using affinity methods as before.[5]

Synthesis. Synthesis, characterization, and pK_a determination of Bzbr analogues **2**−**16** was previously described.[5,13] Compounds **17** and **18** were characterized using a 300 MHz Varian Mercury NMR spectrometer (Palo Alto, CA) and LC/MS/MS (LCQ Advantage, Thermo Electron Corp., San Jose, CA). The purity of both compounds **17** and **18** were confirmed by HPLC in two different systems. The conditions and HPLC traces are provided as Supporting Information.

(3-Methoxyphenyl)-(2-methylbenzofuran-3-yl)methanone-$^2H_3$ (17). Analogue **11** (1.0 mmol) [13] was added to 9 mL of anhydrous THF containing 1 mL of DMF at 4 °C. Sodium hydride dispersion (1.2 equiv) that had been previously washed with hexanes and kept under argon was then added. Iodomethane-$^2H_3$ (99.5% enriched, 10 equiv) was then introduced slowly by syringe and stirred for 1 h at which point the reaction was quenched with 1 mL of methanol. After removal of solvent in vacuo, the sample was run over a bed of silica with 5% ethyl acetate in hexanes and eluted as a yellow oil. Isolated yield: 39%. ^{1}H NMR ($CDCl_3$): δ = 2.55 (s, 3H), 7.20 (m, 3H, ArH), 7.37 (m, 3H, ArH), 7.45 (m, 2H, ArH). ^{13}C NMR ($CDCl_3$): δ = 15.0, 21.9, 111.1, 113.4, 117.2, 119.4, 121.6, 122.0, 123.8, 124.7, 127.1, 129.8, 140.9, 153.9, 160.0, 162.2, 192.0. ESI-MS: *m/z* = 270.4 (M + H$^+$), 159.1 (M − 110, 100), 138.1 (M − 131, 39) at 40% ionization energy.

(3,5-Dibromo-4-hydroxyphenyl)-[2-(1-hydroxyethyl)-benzofuran-3-yl]methanone (18). First, 0.25 mmol of Bzbr protected as an acetate at the phenol was added to 1.2 equiv of *N*-bromosuccinimide and 0.1 equiv of AIBN in 20 mL of CCl_4 and heated to reflux for 4 h to form the 1′-bromo compound. Bromine displacement was next carried out in 10 mL of DMF with 5 equiv of cesium acetate at 23 °C for 24 h after which the solvent was removed by vacuum. These first two steps essentially went to completion based on TLC. The diester compound was then hydrolyzed with anhydrous potassium carbonate (5 equiv) in methanol for 12 h at 23 °C and concentrated. Finally, the sample was subjected to preparative TLC using 5% methanol in methylene chloride to develop the plate and give the C-1′ alcohol of Bzbr. Isolated yield: 17% ^{1}H NMR ($CDCl_3$): δ = 1.71 (d, 3H), 5.14 (q, 1H), 7.23 (m, 3H, ArH), 7.37 (m, 1H, ArH), 7.58 (d, 1H, ArH), 8.04 (s, 2H, ArH).

^{13}C NMR ($CDCl_3$): δ = 20.3, 63.7, 110.4, 112.2, 116.4, 121.4, 124.4, 125.7, 125.9, 133.0, 134.1, 153.7, 153.9, 166.9, 188.9. ESI-MS: m/z = 439.2 ($M - H^+$), 251.0 ($M - 189$, 42) at 40% ionization energy.

Enzyme Reconstitution and 3-*O*-Methylfluorescein (MFL) Assay. Purified, recombinant 2C19 was reconstituted with purified cytochrome P450 reductase and cytochrome b5 into unilamellar liposomes of dilauroylphosphatidylcholine (DLPC) exactly as before.[5] Reactions were carried out in a 1.5 mL polypropylene microcentrifuge tube with different concentrations of MFL at 3−6 fixed amounts of inhibitor (in methanol) with 2.5 pmol of the reconstituted 2C19, an NADPH regenerating system (2 mM $MgCl_2$, 10 mM glucose-6-phosphate, 1 mM NADP, 1 U of glucose-6-phosphate dehydrogenase), and 1000 U of catalase in 50 mM potassium phosphate buffer (pH 7.4) at a final volume of 0.2 mL. The stock solution of MFL was prepared to be 0.2 mM by sonicating the MFL with 1 equiv of potassium hydroxide in water. The reactions were allowed to continue for 20 min in a shaking water bath maintained at 37 °C. Acetonitrile (0.2 mL) containing 100 pM dichlorofluorescein (DCFL, internal standard) was then used to quench the incubations. The sample tubes were subsequently centrifuged at 12 000*g* for 20 min so the precipitated protein components could be discarded.

Separation of fluorescein was carried out using HPLC (Agilent Zorbax XDB−C8, 4.6 × 150 mm, 5 μm) using potassium phosphate at pH 8.0 (A) and acetonitrile (B). The samples were injected onto the column equilibrated at 95% A/5% B whereupon a gradient was immediately initiated to reach 65% A/35% B over 9 min and held at this ratio for an additional 4 min. A Hitachi (San Jose, CA) L-7480 fluorescence detector was used to quantitate fluorescein based upon a standard curve with the excitation and emission wavelengths set to 495 and 525 nm, respectively. Retention times were as follows: FL, 9.0 min, DCFL, 10.2 min, and MFL, 12.8 min.

Metabolism of Bzbr (1), and Its Dimethylphenol (2) and 3″-Methoxy (16, 17) Analogues. Reconstituted 2C19 and 2C9 were incubated with 25 μM Bzbr (**1**) and its dimethyl analogue **2** for 30 min in 50 mM potassium phosphate, pH 7.4, after initiating the reactions with 1 mM NADPH. Substrates were dissolved in methanol to make 5 or 10 mM stock solutions. Hydrochloric acid (3 M, 0.2 mL) was used to quench the reactions, and 50 pmol of warfarin was added as internal standard before the products were extracted into 6 mL of chloroform. After being dried over $MgSO_4$, the samples were concentrated under nitrogen and dissolved in 200 μL of methanol for LC/MS analysis. The HPLC method used a C-18 column (Agilent Hypersil BDS, 2.0 × 125 mm) and a solvent system of 0.1% acetic acid (C) and methanol with 0.1% acetic acid (D) with a flow rate of 0.2 mL/min. Initial conditions consisting of 60% C/40% D were developed to 20% C/80% D from t = 0 to t = 15 min and held at this solvent ratio for 10 additional minutes to elute the remaining substrate. A PDA detector was used to monitor the UV traces at 282 nm.

Metabolism of **16** and **17** was carried with the following changes. Substrate concentration was increased to 50 μM, incubations lasted 60 min, 4′OH-warfarin was used as an internal standard, and mobile phase solvent D was increased to only 65% over the same time course used for Bzbr. Incubations containing both **2** and **16** had these substrate concentrations at 25 and 50 μM, respectively. Retention times under the described conditions were: 4′OH-warfarin, 12.8 min, warfarin, 14 min, dimethylphenol **2**, 20 min, Bzbr (**1**), 25 min, and 3″-methoxy analogue **16**, 27.4 min. Details of metabolites are described in the Results section.

All mass spectrometry was carried out with a Thermo Finnigan LCQ Advantage (Thermo Electron Corp., San Jose, CA) first in full scan mode and then in selected ion monitoring mode to see if any minor hydroxylated metabolites (M + 16) could be detected. No dihydroxylated products were detected in full scan mode, but SIM mode was not used to rule out the existence of such metabolites. After selecting the metabolite parent ions ((M + 1) or (M − 1)) with m/z widths of 1 amu, MS/MS experiments were then conducted under both polarity modes and a range of collision energies. Final collision energies were 40% for Bzbr, the dimethylphenol, and the 3″-methoxy analogue in positive mode and 60% for the dimethyl analogue in negative mode.

Comparative Molecular Field Analysis (CoMFA) Modeling. CoMFA is a ligand-based predictive software with the ability to derive three-dimensional quantitative structure−activity relationships (3D-QSARs). Using regression analysis on the charges for each atom of each molecule in a 3-D aligned library, CoMFA can correlate electrostatic and steric properties with activities (e.g. K_i values) obtained by experiment. Two utilities of CoMFA analysis are its use as a predictive tool to predict K_is (or other properties) of other ligands and contour plots that allow the visualization of predicted favorable and unfavorable properties of the ligands in 3-D. Generally, these plots can be directly translated to interactions with the enzyme, allowing a more directed route of ligand design that exploits the desired properties.

All methods required to use Bzbr analogues in CoMFA analysis were previously described in greater detail for the 2C9 model.[13] This includes Bzbr ligand alignment, minimization, and calculation of MNDO partial charges using the MOPAC module within SYBYL v6.6.[31] The Bzbr analogues were then added to a new molecular spreadsheet containing the reciprocal $\ln(-K_i)$ values determined for 2C19 experimentally. All CoMFA analysis used the default parameters of 30 kcal/mol electrostatic and steric cutoffs, and leave-one-out cross-validation with 2.0 kcal/mol column filtering was used in all cases.

Bzbr ligands were aligned to the phenobarbital, nirvanol, and phenytion analogues used in our previous 2C19 CoMFA models [15] in four distinct ways. The first two methods fashioned the two sites of metabolism for analogue **2** to overlie the metabolized position of the most potent phenobarbital analogue, (−)-*N*-3-benzylphenobarbital, whose structure is in Figure 6. The remaining aromatic ring was then aligned with the benzyl group of (−)-*N*-3-benzylphenobarbital. Figure 5a and 5b illustrate these two alignments. The third and fourth alignments that are not presented placed the Bzbr benzofuran in the plane of the barbiturate ring or rotated the template benzyl ring 180°. For the latter, this placed the nonmetabolized ring position for both compounds at the other face of the barbiturate ring.

Acknowledgment. We thank Jan Wahlstrom for detailing the synthetic scheme for 1′-OH Bzbr and suggesting target Bzbr analogues, and Tamara Dowers, Greg Crouch, and Josh Alfaro for technical help. This research was supported by NIH research grants GM032165 and ES009122.

Supporting Information Available: HPLC traces of compounds **17** and **18** are available. This material is free of charge via the Internet at http://pubs.acs.org.

References

(1) Miners, J.; Birkett, D. Cytochrome P4502C9: an enzyme of major importance in human drug metabolism. *Br. J. Clin. Pharmacol*. **1998**, *45*, 525−538.
(2) Rettie, A.; Korzekwa, K.; Kunze, K.; Lawrence, R.; Eddy, A.; Aoyama, T.; Gelboin, H.; Gonzalez, F.; Trager, W. Hydroxylation of warfarin by human cDNA-expressed cytochrome P-450: a role for P-4502C9 in the etiology of (S)-warfarin-drug interactions. *Chem Res Toxicol*. **1992**, *5*, p 54−59.
(3) Mancy, A.; Dijols, S.; Poli, S.; Guengerich, P.; Mansuy, D. Interaction of sulfaphenazole derivatives with human liver cytochromes P450 2C: molecular origin of the specific inhibitory effects of sulfaphenazole on CYP 2C9 and consequences for the substrate binding site topology of CYP 2C9. *Biochemistry* **1996**, *35* (50), p 16205−16212.
(4) Takahashi, H.; Sato, T.; Shimoyama, Y.; Shioda, N.; Shimizu, T.; Kubo, S.; Tamura, N.; Tainaka, H.; Yasumori, T.; Echizen, H. Potentiation of anticoagulant effect of warfarin caused by enantioselective metabolic inhibition by the uricosuric agent benzbromarone. *Clin Pharmacol Ther*. **1999**, *66* (6), 569−581.

(5) Locuson, C. W., II.; Wahlstrom, J. L.; Rock, D. A.; Rock, D. A.; Jones, J. P. A new class of CYP2C9 inhibitors: probing 2C9 specificity with high-affinity benzbromarone derivatives. *Drug Metab Dispos*. **2003**, *31* (7), 967−971.
(6) Goldstein, J. A.; Faletto, M. B.; Romkes-Sparks, M.; Sullivan, T.; Kitareewan, S.; Raucy, J. L.; Lasker, J. M.; Ghanayem, B. I. Evidence that CYP2C19 is the major (*S*)-mephenytoin 4′-hydroxylase in humans. *Biochemistry* **1994**, *33* (7), 1743−1752.
(7) Suzuki, H.; Kneller, M. B.; Haining, R. L.; Trager, W. F.; Rettie, A. E. (+)-N-3-benzyl-nirvanol and (−)-N-3-benzyl-phenobarbital: new potent and selective in vitro inhibitors of CYP2C19. *Drug Metab. Dispos*. **2002**, *30*, 235−239.
(8) Desta, Z.; Zhao, X.; Shin, J.-G.; Flockhart, D. A. Clinical significance of the cytochrome P450 2C19 genetic polymorphism. *Clin Pharmacokinet*, **2002**, *41* (12), 913−958.
(9) Gotoh, O. Substrate recognition sites in cytochrome P450 family 2 (CYP2) proteins inferred from comparative analyses of amino acid and coding nucleotide sequences. *J. Biol. Chem*. **1992**, *267* (1), 83−90.
(10) Ibeanu, G. C.; Ghanayem, B. I.; Linko, P.; Li, L.; Pedersen, L. G.; Goldstein, Identification of residues 99, J. A.;220, and 221 of human cytochrome P450 2C19 as key determinants of omeprazole hydroxylase activity. *J. Biol. Chem*. **1996**, *271* (21), 12496−12501.
(11) Tsao, C.; Wester, M.; Ghanayem, B.; Coulter, S.; Chanas, B.; Johnson, E.; Goldstein, J. Identification of human CYP2C19 residues that confer S-mephenytoin 4′-hydroxylation activity to CYP2C9. *Biochemistry* **2001**, *40*, 1937−1944.
(12) Dickmann, L. J.; Locuson, C. W., II.; Jones, J. P.; Rettie, Differential roles of R97, A. E.; D293, and R108 in enzyme stability and substrate specificity of CYP2C9. *Mol. Pharmacol*. **2004**, *65*, 842−850.
(13) Locuson, C. W., II.; Rock, D. A.; Jones, J. P. Quantitative binding models for CYP2C9 based on benzbromarone analogues. *Biochemistry* **2004**, *43*, 6948−6958.
(14) Rock, D. A.; Perkins, B. N.; Wahlstrom, J.; Jones, J. P. A method for determining two substrates binding in the same active site of cytochrome P450 μ_B3: an explanation of high energy omega product formation. *Arch Biochem Biophys*, **2003**, *416* (1), 9−16.
(15) Suzuki, H.; Kneller, M. B.; Rock, D. A.; Jones, J. P.; Trager, W. F.; Rettie, A. E. Active-site characteristics of CYP2C19 probed with novel inhibitors: development of an integrated CoMFA-homology model. *Arch. Biochem. Biophys.* **2004**, in press.
(16) Marques-Soares, C.; Dijols, S.; Macherey, A. C.; Wester, M. R.; Johnson, E. F.; Dansette, P. M.; Mansuy, D. Sulfaphenazole derivatives as tools for comparing cytochrome P450 2C5 and human cytochromes P450 2Cs: identification of a new high affinity substrate common to those enzymes. *Biochemistry* **2003**, *42* (21), 6363−6369.
(17) Abelo, A.; Andersson, T. B.; Antonsson, M.; Naudot, A. K.; Skanberg, I.; Weidolf, L. Stereoselective metabolism of omeprazole by human cytochrome P450 enzymes. *Drug Metab. Dispos*. **2000**, *28* (8), 966−972.
(18) Kim, K. A.; Kim, M. J.; Park, J. Y.; Shon, J. H.; Yoon, Y. R.; Lee, S. S.; Liu, K. H.; Chun, J. H.; Hyun, M. H.; Shin, J. G. Stereoselective metabolism of lansoprazole by human liver cytochrome p450 enzymes. *Drug Metab. Dispos*. **2003**, *31* (10), 1227−1234.
(19) Williams, P. A.; Cosme, J.; Ward, A.; Angove, H. C.; Matak Vinkovic, D.; Jhoti, H. Crystal structure of human cytochrome P450 2C9 with bound warfarin. *Nature* **2003**, *424* (6947), 464−468.
(20) Payne, V. A.; Chang, Y. T.; Loew, G. H. Homology modeling and substrate binding study of human CYP2C18 and CYP2C19 enzymes. *Proteins* **1999**, *37*, 204−217.
(21) Lewis, D. F. V. Modelling human cytochromes P450 involved in drug metabolism from the CYP2C5 crystallographic template. *J. Inorg. Biochem*. **2002**, *91*, 502−514.
(22) Jung, F.; Griffin, K. J.; Song, W.; Richardson, T. H.; Yang, M.; Johnson, Identification of amino acid substitutions that confer a high affinity for sulfaphenazole binding, E. F.; a high catalytic efficiency for warfarin metabolism to P450 2C19. *Biochemistry* **1998**, *37*, 16270−16279.
(23) Niwa, T.; Kageyama, A.; Kishimoto, K.; Yabusaki, Y.; Ishibashi, F.; Katagiri, Amino acid residues affecting the activities of human cytochrome P450 2C9, M.; 2C19. *Drug Metab. Dispos*. **2002**, *30* (8), 931−936.
(24) De Vries, J.; Walter-Sack, I.; Voss, A.; Forster, W.; Ilisistegui Pons, P.; Stoetzer, F.; Spraul, M.; Ackermann, M.; Moyna, G. Metabolism of benzbromarone in man: structures of new oxidative metabolites, 6-hydroxy- and 1′-oxo-benzbromarone, and the enantioselective formation and elimination of 1′-hydroxybenzbromarone. *Xenobiotica* **1993**, *23* (12), 1435−1450.
(25) Higgins, L.; Korzekwa, K. R.; Rao, S.; Shou, M.; Jones, J. P. An assessment of the reaction energetics for cytochrome P450-mediated reactions. *Arch. Biochem. Biophys*. **2001**, *385* (1), 220−30.
(26) Jones, J. P.; Korzekwa, K. R.; Rettie, A. E.; Trager, Isotopically sensitive branching, W. F.; its effect on the observed intramolecular isotope effects in cytochrome P-450 catalyzed reactions: a new method for the estimation of instrinsic isotope effects. *J. Am. Chem. Soc.* **1986**, *108*, 7074−7078.
(27) Rock, D. A.; Boitano, A. E.; Wahlstrom, J. L.; Jones, J. P. Use of kinetic isotope effects to delineate the role of phenylalanine 87 in P450(BM-3). *Bioorg. Chem*. **2002**, *30* (2), 107−18.
(28) Miwa, G. T.; Garland, W. A.; Hodshon, B. J.; Lu, A. Y. H.; Northrop, D. B. Kinetic isotope effects in cytochrome P-450-catalyzed oxidation reactions. Intermolecular and intramolecular deuterium isotope effects during the N-demethylation of N,N-dimethylphentermine. *J. Biol. Chem*. **1980**, *255*, 6049−6054.
(29) Korzekwa, K. R.; Gillette, J. R.; Trager, W. F. Isotope effect studies on the cytochrome P450 enzymes. *Drug Metab. Rev*. **1995**, *27* (1−2), 45−59.
(30) Iyer, K. R.; Jones, J. P.; Darbyshire, J. F.; Trager, W. F. Intramolecular isotope effects for benzylic hydroxylation of isomeric xylenes and 4,4′-dimethylbiphenyl by cytochrome P450: Relationship between distance of methyl groups and masking of the intrinsic isotope effect. *Biochemistry* **1997**, *36* (23), 7136−7143.
(31) *SYBYL*, Tripos Inc., v6.6: St. Louis, MO.

JM049605M